Corrosion preserving high density plasma treatment of precipitation hardening stainless steel

Iñigo Braceras, Iñigo Ibáñez, Santiago Domínguez-Meister, Aiala Urgebain, Jose Angel Sánchez-García, Aitor Larrañaga, Iñaki Garmendia

PII: S0257-8972(18)30044-6
DOI: https://doi.org/10.1016/j.surfcoat.2018.01.036
Reference: SCT 23019

To appear in: *Surface & Coatings Technology*

Received date: 30 October 2017
Revised date: 22 December 2017
Accepted date: 11 January 2018

Please cite this article as: Iñigo Braceras, Iñigo Ibáñez, Santiago Domínguez-Meister, Aiala Urgebain, Jose Angel Sánchez-García, Aitor Larrañaga, Iñaki Garmendia , Corrosion preserving high density plasma treatment of precipitation hardening stainless steel. The address for the corresponding author was captured as affiliation for all authors. Please check if appropriate. Sct(2017), https://doi.org/10.1016/j.surfcoat.2018.01.036

Corrosion Preserving High Density Plasma Treatment of Precipitation Hardening Stainless Steel

Iñigo Braceras[a], Iñigo Ibáñez[a], Santiago Domínguez-Meister[a], Aiala Urgebain[a], Jose Angel Sánchez-García[a], Aitor Larrañaga[b] and Iñaki Garmendia[c]

a) Tecnalia Research & Innovation, Mikeletegi Pasealekua 2, Donostia - San Sebastián, Spain.

b) Tratamientos Térmicos TTT, S.A., Bergara, Spain.

c) University of the Basque Country UPV/EHU, Mechanical Engineering Department, Donostia-San Sebastián, Spain

Corresponding author.

Iñigo Braceras

Postal address: Mikeletegi Pasealekua 2, 20009 Donostia - San Sebastián, Spain.

e-mail: inigo.braceras@tecnalia.com

Tel.: +34 946 430 850

Abstract.

Specialty alloys such as precipitation hardening stainless steels are routinely used in critical applications requiring high strength and corrosion resistance, e.g. in aeronautics, in ground transportation and the biomedical field. Nonetheless, their tribological properties remain poor, while the application of surface treatments results in loss of corrosion resistance. Therefore, typically a not fully satisfactory compromise must be adopted.

In the present work, the improvement of tribological features, without loss of corrosion resistance, of the 1.4545 (15-5PH) steel has been explored with the use of high density plasmas. The work has focused on long cylindrical geometries, close to those of real applications.

The microstructure and composition of the treated surfaces were studied and the corresponding corrosion resistance stablished. The characteristics of the high density plasmas as well as the sample disposition were key factors in the outcomes, which ranged from fully corroded to corrosion resistant surfaces. Results also showed in certain cases the high density plasmas causing surface cracks followed by local corrosion.

Additionally tribological studies demonstrated improvement in wear resistance, and Electrical Contact Resistance (ECR) was found to be a good indicator of the wear phenomena occurring along the tests. An equivalent electric circuit is proposed. Actually ECR could be a useful and simple way of monitoring the surface status and assist in assuring safe and dependable operational lives of the components.

In conclusion, treatment conditions of cylindrical 1.4545 (15-5PH) have been defined, which provide with an improved tribological performance, preserving corrosion resistance, with ECR a useful performance monitoring parameter.

Keywords: plasma natriding, active screen, hollow cathode, 15-5PH, martensitic stainless steel, corrosion.

3. Text

1. Introduction

In many critical applications, in the aeronautical (e.g. landing gear components), ground transportation (e.g. load sensing components) and biomedical (e.g. surgical tools) fields, good mechanical and tribological properties are required together with a good corrosion resistance and no delamination risk whatsoever if a coating is present. In such cases, precipitation hardening martensitic stainless steels are often the material of choice. Plasma nitriding is a well know industrial process, which can improve surface properties of many steels. Nevertheless, preserving the corrosion resistance of stainless steels, especially martensitic stainless steels, while producing hardened surfaces with good tribological properties, typically leads to not fully satisfactory compromises [1]. Relatively little research has been carried out on the effect of plasma nitriding on martensitic precipitation hardening stainless steel. Some good results were found regarding surface hardness and α'_N (nitrogen supersaturated expanded martensite) layer thickness, but often with poor corrosion behavior because of the formation of chromium nitrides during the plasma nitriding process [2,3,4,5,6,7,8,9].

On the other hand, active screen plasma nitriding offers a number of advantages over conventional plasma nitriding. The active screen acts as both a generator of plasma species and source of radiation that acts as a heater, thus enabling a better process temperature control, independent from the voltage bias applied to the treated part. Likewise, the hollow cathode effect produces denser plasmas, by means of the "pendulum", photoionization and stepwise ionization [10]. The combination of both has been studied recently on austenitic stainless steel, aiming at rapid nitriding processes in short times [11,12,13,14,15].

In this work, the combination of the active screen plasma nitriding and hollow effect

has been explored on the 1.4545 grade (15-5PH) martensitic stainless steel, on long cylindrically shaped geometries, aiming at achieving a thick nitride layer (above 50µm) with a good compromise between tribological properties and corrosion resistance (> 48h at Salt Spray Test (SST)).

2. Material and methods

The active screen plasma nitriding technique in combination with the hollow cathode effect was used in this work. In the active screen plasma treatments, the outer screen is subjected to a voltage, while the samples are immersed in plasma and biased to a lower potential. Furthermore, if the sample is surrounded by an open ended tube, in some cases, the hollow cathode occurs inside such a tube. A schematic of the technique used for the plasma treatments is shown in Fig. 1. In this work the screen and the part were each connected to independent DC power supplies.

The samples used in this work were 10 mm in diameter and 80 mm long, manufactured on grade 1.4545.3 stainless steel (15-5PH in the H1100 condition (AMS5659)), with a surface finishing of Ra 1.0 μm. Its chemical composition is (%): C≤ 0.07, Si≤ 1.00, Mn≤ 1.00, P≤ 0.03, S ≤ 0.015, Cr 15.0-15.5, Mo≤ 0.50, Ni 3.00-5.50, Cu 2.50-4.50, Nb≥ 5xC. The surrounding tube, manufactured on austenitic stainless steel, AISI 316L, was 45mm in diameter, 120 mm long, and open ended in both ends.

The samples were initially plasma cleaned with 50/50 Ar/H_2 for a minimum of 1h to remove residual surface contaminants and the naturally occurring surface oxides, using a bias voltage of 250 V (and 210 V in the screen). The surface treatments were subsequently applied at a pressure of 120 Pa, with a gas mixture of 75/25 H_2/N_2, according to the parameters detailed in Table 1. The process temperatures were monitored by a thermocouple in an adjoining bulk dummy cylinder, and later in the study also by one in the tube surrounding the sample. After the treatment, the samples cooled in vacuum down to room temperature.

Nitride layer thickness was measured by optical microscopy (Nikon Eclipse MA200 and Olympus BX51M), once sectioned for metallographic examination and etched (Beraha). Additionally, cross sections were analyzed by Scanning electron Microscopy (SEM)

and Energy Dispersive Spectroscopy (EDS) (JEOL JSM-5910LV), before and after etching. Surface structure was analyzed by X-Ray Diffraction (XRD) (D8 Advance, Bruker) by using Cu-Kα radiation (λ= 1.544 Å) at glancing angle of incidence of 2º. The corrosion resistance was assessed in Salt Spray Tests (SST) performed following the ISO 9297 standard [16]. ~~The limitations of accelerated corrosion testing are well known, specifically concerning salt spray tests. The standard itself mentions that there is seldom a direct relation between resistance to the action of salt spray and resistance to corrosion in other media, and therefore, the test results should not be regarded as a direct guide to the corrosion resistance in all environments. Nevertheless, the method gives a means of checking that the comparative quality of a metallic material, with or without corrosion protection, is maintained. Thus, this test method was selected to assess the damage inflected in the substrate material by the plasma nitriding treatment and because, despite all the limitations, it is still widely used in a number of industrial fields.~~

The coefficient of friction (COF) and electrical contact resistance (ECR) were measured in cylinder on cylinder reciprocating tests (MT4002 MICROTEST tribometer), at different loads (5 and 15N), low and high humidity (18% and 80% RH respectively), mean speed of 0.020 m/s and at room temperature. One of the cylinders had either plasma treated or an untreated surface, and the other had an untreated surface. Wear tracks were assessed by optical microscopy and Scanning Electron Microscopy / Energy Dispersive Spectroscopy.

3. Results

3.1. Process parameters, corrosion resistance and nitride layer thickness

Conventional plasma nitriding treatments, i.e. with no surrounding tube and thus no hollow cathode effect, produced thin nitride layers, 4 and 8 μm thick respectively for 5 and 25 h treatment times at 350 ºC (Ref. #350.5 and #350.25; Table 1; Fig. 2 a and b respectively). These surfaces already showed red rust at the SST tests at 4h (Fig. 3).

On the other hand, the same process time and temperature accompanied by the hollow cathode effect showed a nitride layer thickness above 100 μm, though also red rust at the SST tests at 4h (Ref. #350HC5).

Milder treatment conditions, in the form of shorter nitriding treatments, 2.5h, did not improve the corrosion resistance (Ref.#350HC2.5). Conversely, treatment at lower temperature, 275 ºC (370ºC at the tube), showed better corrosion resistance with sections of the surface showing resistance after 48h at SST, though others showed red rust before 4h (Ref.#275HC5). In both treatments, radial cracks were detected at the surface, which presented a nitride layer thickness of 140 and 155 μm respectively (Ref. #350HC2.5 and 275HC5).

At even milder conditions, 2.5h and 275 ºC (350º at the tube), the nitride layer thickness was reduced to ~100μm, with further improvement of the corrosion resistance, but still presence of cracks (Ref. #275HC2.5).

At slightly higher temperature but shorter treatment time, 1h and 270 ºC (365º at the tube), the nitride layer thickness was not reduced, ~ 60μm, while the SST test showed a corrosion resistance above 240h (Ref. ##275HC1).

Overall, when measured, it was observed that the presence of the hollow cathode effect produced an increase in the temperature of 75 to 95ºC in the surrounding tube comparing with the adjoining cylindrical dummy.

3.2. Surface structure

Selected surface cross sections were analyzed by EDS and phases present at the surface by XRD, to learn about the reasons behind the remarkable differences in corrosion resistance.

EDS

Big differences in corrosion resistance were observed in references #350HC2.5 and #275HC5, which presented quite similar nitride layer thicknesses. Therefore, these surfaces were analyzed in detail by SEM and EDS, together with ref. #275HC1.

EDS showed the same initial elemental composition in all references (Fig. 4, <). On the other hand, after surface etching, differences appeared: while ref. #350HC2.5 showed an increasing displacement of Cr concentration towards the surface (Fig. 4, yellow line, a,>), ref. #275HC5showed an intermediate region with lower Cr content (Fig. 4, yellow line, b,>), and ref. #275HC1 showed no apparent change (Fig. 4, yellow line, c,>).

XRD

XRD spectra of ref #275HC5, #350HC2.5, #275HC1 the untreated steel are shown in Fig. 5. These surfaces, which have showed remarkably different corrosion resistances, also presented differences in the XRD spectra.

The untreated surface presented a single diffraction peak of the martensite phase (α′Fe) (Fig. 5). CrN and α'_N peaks were much lower in the case of reference #275HC1 as compared with #350HC2.5, and even lower for ref. #275HC1 [7].

3.3. Electro-tribology studies

Tribology studies were performed with the surface showing better corrosion resistance (#275HC1) and control untreated surfaces, at different loads (5 and 15N) and humidity (18 and 80 %RH), on a cylinder on cylinder reciprocating configuration. Both the coefficient of friction (COF) and electrical contact resistance (ECR) were monitored along the tests (Fig. 6).

The 1.4545 (15-5PH) against 1.4545 (15-5PH) pair at low humidity showed two distinct patterns: first low friction and high ECR, then higher COF and low ECR (Fig. 6, a). In the case of the 1.4545 (15-5PH) against plasma nitrided #275HC1 pair, the ECR remained low and the COF rose to high values faster (Fig. 6, b).

At larger loads, results were similar, but the second region of higher COF occurred before, with less test cycles (Fig. 6, c and d).

Conversely, at high humidity, the 1.4545 (15-5PH) against 1.4545 (15-5PH) pair showed low ECR but increasing COF, while the 1.4545 (15-5PH) against plasma nitrided #275HC1 pair still showed high COF and two distinct regions of ERC values (Fig. 6, e and f).

Finally, as part of the study, an equivalent electric circuit has been proposed (Fig. 7).

4. Discussion.

Results show that process temperature, duration and plasma density are key parameters in the resulting nitride layers and their performance. Conventional plasma treatments typically applied on stainless steels, i.e. at 350ºC process temperature, produce a very thin nitride layer (ref. #350.5: 4µm), even if the process duration is prolonged (ref. #350.25: 8µm). Increasing treatment time produces diminishing increases in the nitride layer thickness. This is in accordance with results reported elsewhere [2,5,6,9]. Besides, it basically destroys the corrosion resistance ability of the alloy.

The hollow cathode effect increases the nitride layer thickness remarkably, i.e. above 100µm. This thickness is much larger than that achieved by Li et al. on stainless steel, albeit with a different configuration [11].

This is due mainly to two related reasons: increase in both the process temperature and the plasma density. The former can be observed on the temperatures measured on the treatment chamber by means of thermocouples in a dummy bulk cylinder and in the tube surrounding the 1.4545 (15-5PH) samples (Table 1), with increases in the range of 75 to 95ºC. The influence of the latter is clear comparing the thicknesses achieved at nitriding temperatures of 350ºC for 5h with conventional plasma and hollow cathode presence: 4µm at ref. #350.5 as compared with 155µm at ref. #275HC5. The increasing nitride layer thickness with increasing N_2 percentage and ion spices in the plasma has actually been reported, though with much thinner thicknesses, $\leq$ 20µm, the opposite effect on corrosion resistance due to Cr_2N formation, and no hollow cathode effect involved [2].

However, the hollow cathode effect does not preclude the precipitation of Cr nitrides, the main reason behind the loss of corrosion resistance. This is clearly evident in surface ref.#350HC2.5, where the XRD spectrum shows presence of peaks corresponding to Cr

nitrides as well as α′N nitrogen supersaturated expanded martensite (Fig. 5), while red corrosion is already present in 4h at the SST (Fig. 3).

However, thanks to the hollow cathode effect, thicker thicknesses can be achieved in shorter treatment times, with potentially less precipitation of Cr nitrides.

This has been observed in the EDS depth profile analyses. Ref #275HC5 shows a lesser increase in the near surface of Cr than ref. #350HC2.5 (Fig. 4, a) after etching, especially in an intermediate region of the nitride layer, possibly indicating a lower degree of precipitates, i.e. chromium nitrides, deleterious for the corrosion resistance, because the degree of free metallic chromium diminishes. Ref. #275HC1 shows actually no such increase. These differences in the severity of the etching can also be observed in the optical microscope (Fig. 2).

Concerning the XRD analysis, Dong et al. already reported in his systematic microstructure characterization of plasma nitrided precipitation hardening PH alloy [6], that surface phase constituents , highly treatment temperature dependent, presented nitrogen supersaturated martensite (α'_N-expanded martensite); Nitrogen S-phase grains, if there is a some pre-existent retained austenite, γ'–Fe_4N compound layer and CrN precipitates. Thus, our results (Fig. 5) of the glancing angle XRD analysis were consistent with several papers that reported that the white layer in nitride martensitic steels is mainly a stressed structure called “expanded martensite” [19–21], where nitrogen is present on interstitial sites of the bcc ferrite tetragonally distorted. On the other hand, the higher the temperature and nitriding time, the more CrN was present, #350HC2.5 >#275HC5 > #275HC1.

Naeem et al. have recently reported in the nitriding of AISI 304 austenitic stainless steel that when cathodic cage diameter is decreased and consequently a more reactive plasma

is generated, a phase transformation from conventionally reported γ_N-phase to iron nitrides ($Fe_{2-3}N$, Fe_4N) occurs without precipitation of chromium nitrides, which is behind the improvement of corrosion resistance [17]. Esfandiari et al. have also reported that formation of γ'-Fe_4N in precipitation hardening stainless steels can enhance their corrosion properties, being a face centred cubic (fcc) phase as in austenite, although they report no γ'-Fe_4N in low temperature nitriding at 350ºC [6].

This interpretation is further confirmed in process ref. #275HC2.5, where the process duration has been halved. In this case, the nitride layer is still relatively thick, ~100µm, and the corrosion resistance is only hindered by the presence of surface cracks (Fig. 2-3). The authors actually explored modifying the heating and cooling speeds to avoid the formation of these cracks (results not reported here), but to no effect.

A further halving of the process duration to 1h and slightly higher temperature, ref. #275HC1, has rendered much improved results: absence of red rust up to 240h at the SST test (Fig. 3), associated with absence of cracks (Fig. 2) and much lower precipitation of Cr (Fig. 5), with still a thick nitride layer, ~ 60 µm.

In conclusion, preserving the corrosion resistance is proven to be associated to the absence of surface cracks and reduced precipitation of chromium nitrides.

Regarding the tribological performance of these surfaces, as mentioned previously, different patterns can be distinguished (Fig. 6). As a general rule, there is an initial rise in COF due to the enlargement of the contact surfaces, including the reduction of the surface roughness. Then typically two different patterns occur.

At low humidity, a relatively steady regime with low COF, <0.3, ensues. It is known that oxidation effects in dry sliding are generally beneficial because they reduce wear by forming compact layers of oxide particles on the surface which act as lubricant.

The 1.4545 (15-5PH) against 1.4545 (15-5PH) pair shows an oscillating ECR. This is also related to the surface oxide layer, continuously thickening and wearing out. At some point, the oxide layer is removed, a rise in COF and drop in ECR follows, and the systems enters into an adhesive wear regime (Fig. 8, a). In the case of the #275HC1 against 1.4545 (15-5PH) pair, the ECR stays permanently very low, because the oxide layer is removed in the very first cycles, and probably also because the nitride layer conserves enough amount of free Cr. This also causes the COF to rise, and adhesive wear (Fig. 8, a) to occur earlier, i.e. by ~200cycles instead of by ~2000-2500 cycles. The regime transition occurs sooner for larger loads, 15N, i.e. almost immediately and by ~600cycles respectively. In both conditions and pairs the COF ends up close to ~0.8. These COF values are in line with values reported elsewhere, albeit not in a like on like configuration [18,19]. This might be associated with metal on metal sliding conditions. These patterns change with high humidity, 80% RH. In the like on like pair, the ECR remains low, while the COF keeps rising. In the case of the #275HC1 against 1.4545 (15-5PH) pair, there is an initial regime, similar to the one at low humidity, i.e. high but steady COF and low ECR. This is followed by a regime with a slightly lager but still steady COF and higher and oscillating ECR. This could be linked to the generation of wear debris that gets oxidized and trapped in the hard #275HC1 surface, unlike in the like on like condition. At high humidity conditions the COF shows lower values than for lower humidity, i.e. close to ~0.7.

Having applied and studied the treatments on cylindrical parts, the steady and relatively high COF could be valuable in applications where rolling between the parts, but not sliding, is desired. Likewise, monitoring of the ECR could provide information concerning the tribological regime of the parts, e.g. persistent presence of high ECR warning of lower COFs and thus higher risk of losing rolling conditions.

Another alternative simplified way of looking at this can be based on the equivalent electric circuit depicted in Fig. 7. Two main components describe here the system: a resistance associated with the contact surface and a resistance associated with the surface oxides, both of which vary along the time. The former varies initially, while flattening one or both of the original cylindrical surfaces occurs. It might also vary at later stages if adhesive wear sticks on the asperities of the harder surface, in this case, the plasma nitrided one: R contact surface (t) = f(roughness(t); adhesive wear (t),…). The latter, associated with oxide layers, represents the balance between the formation and wear out of oxides (or nitrides), which depends on the sliding conditions, and where both load and humidity might play a relevant role: R oxides (t) = f(contact pressure; humidity,…).

5. Conclusions.

Based on the experimental results obtained in this work, several conclusions can be drawn. The combination of active screen plasma nitriding with the hollow cathode effect produces thicker nitride layers as compared with conventional plasma nitriding. When the plasma density is high, the process duration short enough, and the process temperature is kept low, thick nitride layers can still retain good corrosion resistance, as measured by SST.

These surfaces present steady and high COF. This could be useful, in applications where rolling regimes are preferred in opposition to sliding regimens. Additionally, continuous or periodic monitoring of the ECR can provide insightful information about the system status, evolution and conditions of the tribological regime.

4. List of references.

1. K.H. Lo, C.H. Shek, J.K.L. Lai, Recent developments in stainless steels, Mat. Sci. Eng. R 65 (2009) 39–104.

2. A. Leyland, D.B. Lewis, P.R. Stevensom, A. Matthews, Low temperature plasma diffusion treatment of stainless steels for improved wear resistance, Surf. Coat. Technol. 62(1–3) (1993) 608-617.

3. A. Barua, H. Kim, I. Lee, Effect of the amount of CH4 gas on the characteristics of surface layers of low temperature plasma nitrided martensitic precipitation-hardening stainless steel, Surf. Coat. Technol. 307 (2016) 1034–1040.

4 Y.Sun, Tribocorrosive behavior of low temperature plasma-nitrided PH stainless steels liding against alumina under linear reciprocation with and without transverse oscillations, Wear 362-363 (2016) 105–113.

5. S. P. Brühl, R. Charadia, S. Simison, D.G. Lamas, A. Cabo, Corrosion behavior of martensitic and precipitation hardening stainless steels treated by plasma nitriding, Surf. Coat. Technol. 204 (2010) 3280–3286.

6. M. Esfandiari, H. Dong, The corrosion and corrosion–wear behaviour of plasma nitrided17-4PH precipitation hardening stainless steel, Surf. Coat. Technol. 202 (2007) 466–478.

7. H. Dong, M. Esfandiari, X.Y. Li, On the microstructure and phase identification of plasma nitrided 17-4PH precipitation hardening stainless steel, Surf. Coat. Technol. 202 (2008) 2969–2975.

8. A. Barua, H. Kim, I. Lee, Effect of the amount of CH_4 gas on the characteristics of surface layers of low temperature plasma nitrided martensitic precipitation-hardening stainless steel, Surf. Coat. Technol. 307 (2016) 1034–1040.

9. C. E. Pinedo, S.I.V. Larrotta, A. S. Nishikawa, H. Dong, X-Y. Li, R. Magnabosco, A. P. Tschiptschin, Low temperature active screen plasma nitriding of 17–4 PH stainless steel, Surf. Coat. Technol. 308 (2016) 189–194.

10. S. Muhl, A. Pérez, The use of hollow cathodes in deposition processes: A critical review, Thin Solid Films 579 (2015) 174–198.

11. Y. Li, S. Zhang, Y. He, L. Zhang, L. Wang, Characteristics of the nitrided layer formed on AISI 304 austenitic stainless steel by high temperature nitriding assisted hollow cathode discharge, Mater. Des. 64 (2014) 527–534.

12. W.J. Yang, M. Zhang, Y.H. Zhao, M.L. Shen, H. Lei, L. Xu, J.Q. Xiao, J. Gong, B.H. Yu, C. Sun, Enhancement of mechanical property and corrosion resistance of 316 L stainless steels by low temperature arc plasma nitriding, Surf. Coat. Technol. 298 (2016) 64–72.

13. L. Shen, L. Wang, J.J. Xu, Plasma nitriding of AISI 304 austenitic stainless steel assisted with hollow cathode effect, Surf. Coat. Technol. 228 (2013) S456–S459.

14. K. Nikolov, K. Bunk, A. Jung, P. Kaestner, G. Br€auer, C.P. Klages, High-efficient surface modification of thin austenitic stainless steel sheets applying short-time plasma nitriding by means of strip hollow cathode method for plasma thermochemical treatment, Vacuum 110 (2014) 106-113.

15. I. Braceras, I. Ibáñez, S. Dominguez-Meister, J.A. Sánchez-García, M. Brizuela, A. Larrañaga, I. Garmendia, Plasma Nitriding of the Inner surface of Stainless Steel Pipes, Surf. Coat. Technol. Submitted simultaneously.

16. ISO 9227. Corrosion tests in artificial atmospheres- Salt Spray Tests. International Organization for Standarization, Geneva, Switzerland, 2012.

17. M. Naeem, M.Shafiq, M.Zaka-ul-Islam, NailaNawaz, J.C.Díaz-Guillén, M. Zakaullah, Effect of cathodic cage size on plasma nitriding of AISI304 steel, Mater. Lett. 181 (2016) 78–81.

18. G. Pantazopoulos, T. Papazoglou, P. Psyllaki, G. Sfantos, S. Antoniou, K. Papadimitriou, J. Sideris, Sliding wear behaviour of a liquid nitrocarburised precipitation-hardening (PH) stainless steel, Surf. Coat. Technol. 187 (2004) 77– 85.

19. E.L. Dalibon, V. Trava-Airoldi, L.A. Pereira, A.Cabo, S.P. Brühl, Wear resistance of nitrided and DLC coated PH stainless steel, Surf. Coat. Technol. 255 (2014) 22–27.

5. Tables

Table I. Plasma process parameters.

Reference	Process Temperature at dummy (ºC)	Process Temperature at the tube (ºC)	Process duration (h)	Nitride layer thickness (µm)
#350.5	350	-	5	4
#350.25	350	-	25	8
#350HC5	350	-	5	100-110
#350HC2.5	350	-	2.5	140
#275HC5	275	370	5	155
#275HC2.5	275	350	2.5	100
#275HC1	275	365	1	60

6. List of figure captions;

Fig. 1. Equipment layout during the plasma treatments.

Fig. 2. Cross sections of references #350.5 (a), #350.25 (b), #350HC2.5 (c), #275HC5 (d), #275HC2.5 (e) and #275HC1 (f).

Fig. 3. Samples Ref. #350HC5 (a), #350HC2.5 (b), #275HC5 (c) and #275HC2.5 (d) at the SST test after 4h, 8h, 24h and 48h, and Ref. #275HC1 (e) after 4h, 8h, 48h and 240h.

Fig. 4. EDS depth profiles of references #350HC2.5 (a), #275HC5 (b) and #275HC1(c), before (<) and after (>) etching: Fe in green and Cr in yellow. SEM images, x500.

Fig. 5. XRD spectra of references: untreated 1.4545 (15-15PH) steel, #275HC5, #350HC2.5 and #275HC1.

Fig. 6. COF (blue; average of 100 data points in dark blue) and ECR (red; average of 100 data points in dark red) of 1.4545 (15-5PH) against 1.4545 (15-5PH) pair and 1.4545 (15-5PH) against ref. #275HC1 pair, at 5N and 18%RH (a and b), 15N and 18%RH (c and d) and 5N and 80%RH (e and f) respectively. Note: no all ECR in the same scale.

Fig. 7. Equivalent electric circuit.

Fig. 8. Wear tracks of untreated 1.4545 (15-5PH; a) and ref. #275HC1 (b), after the tribology tests at 5N and 18%RH.

7. Figures.

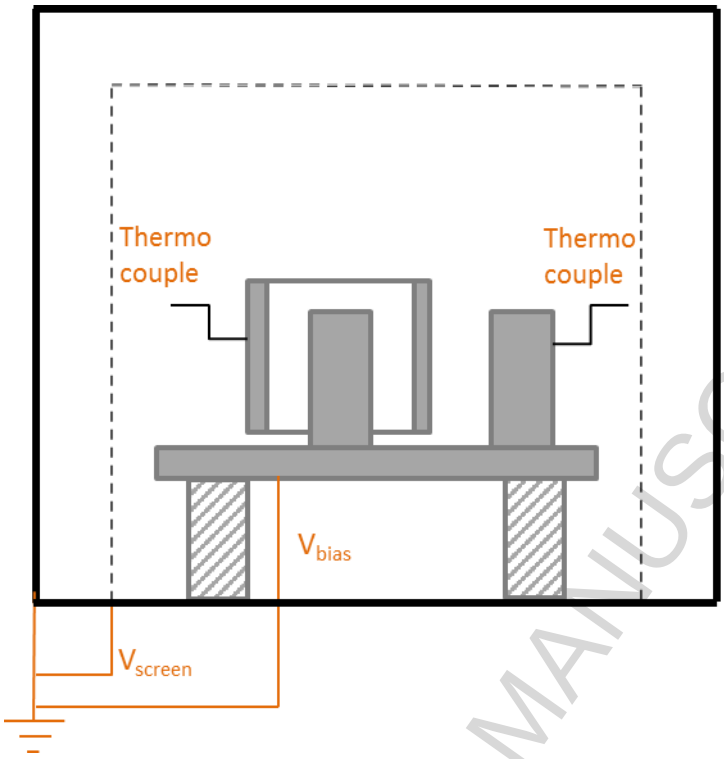

Fig. 1.

a) 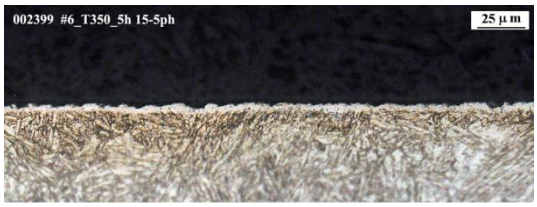

b) 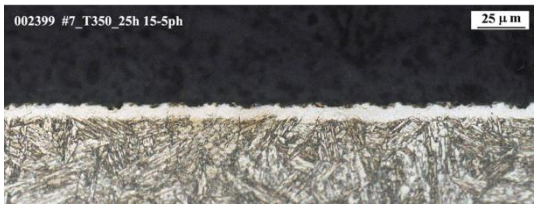

c) 

d) 

e) 

f) 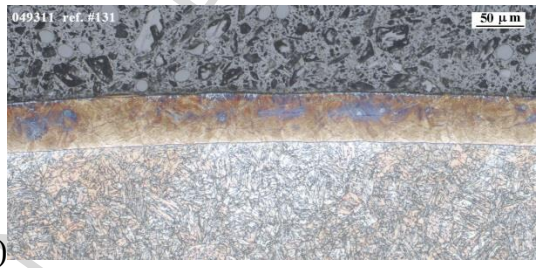

Fig. 2.

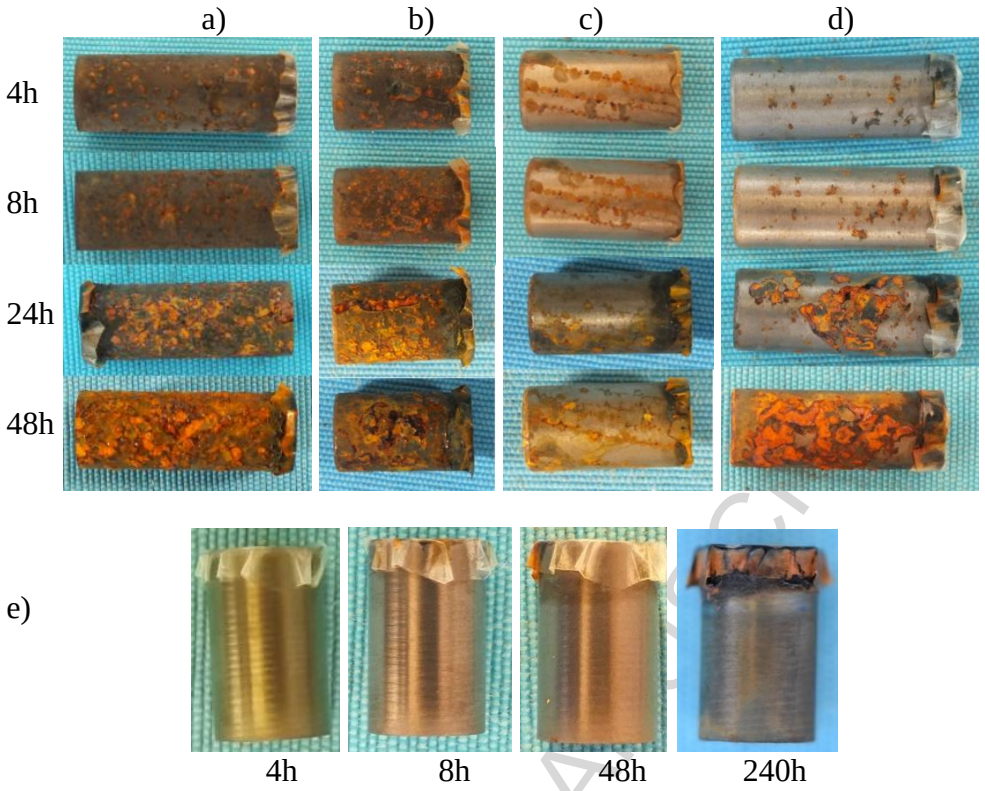

Fig. 3.

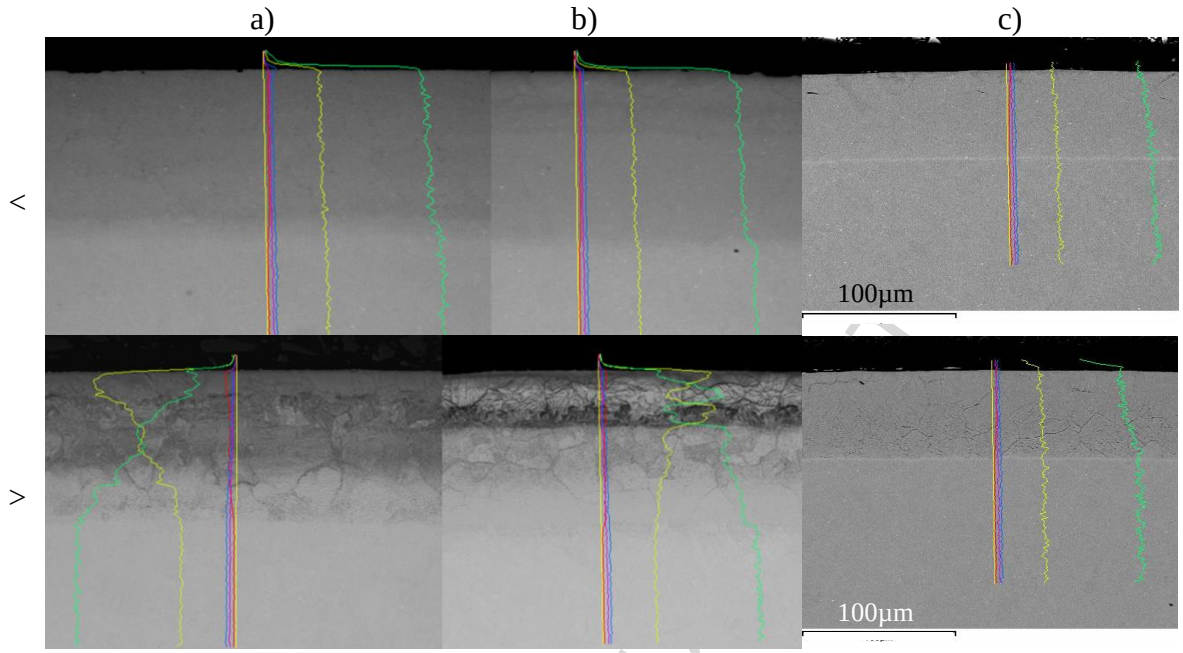

Fig. 4.

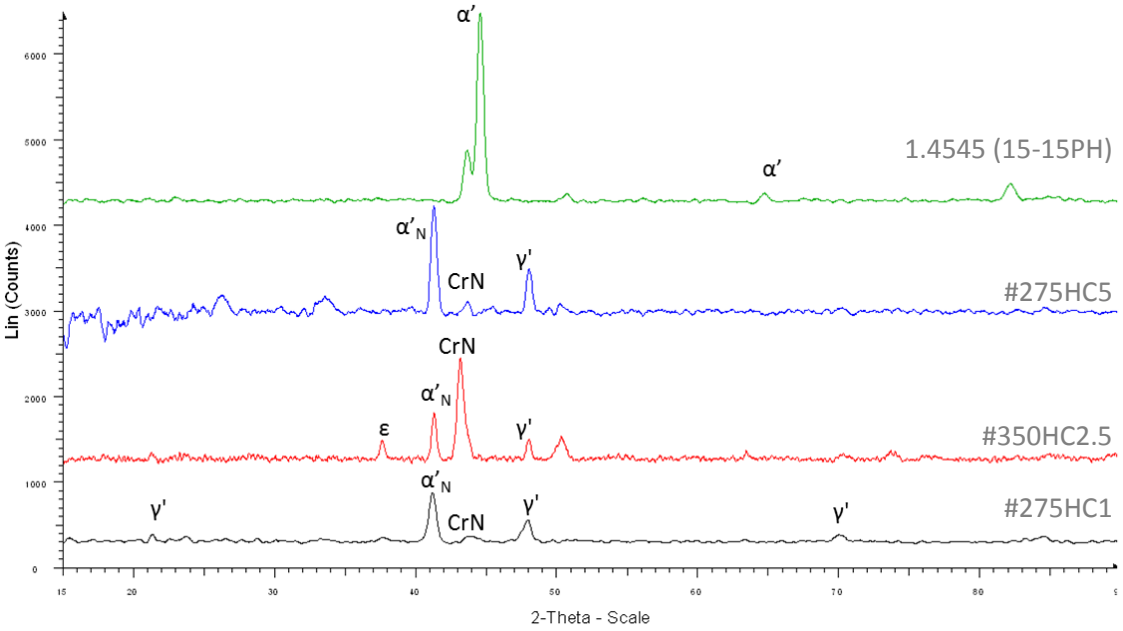

Fig. 5.

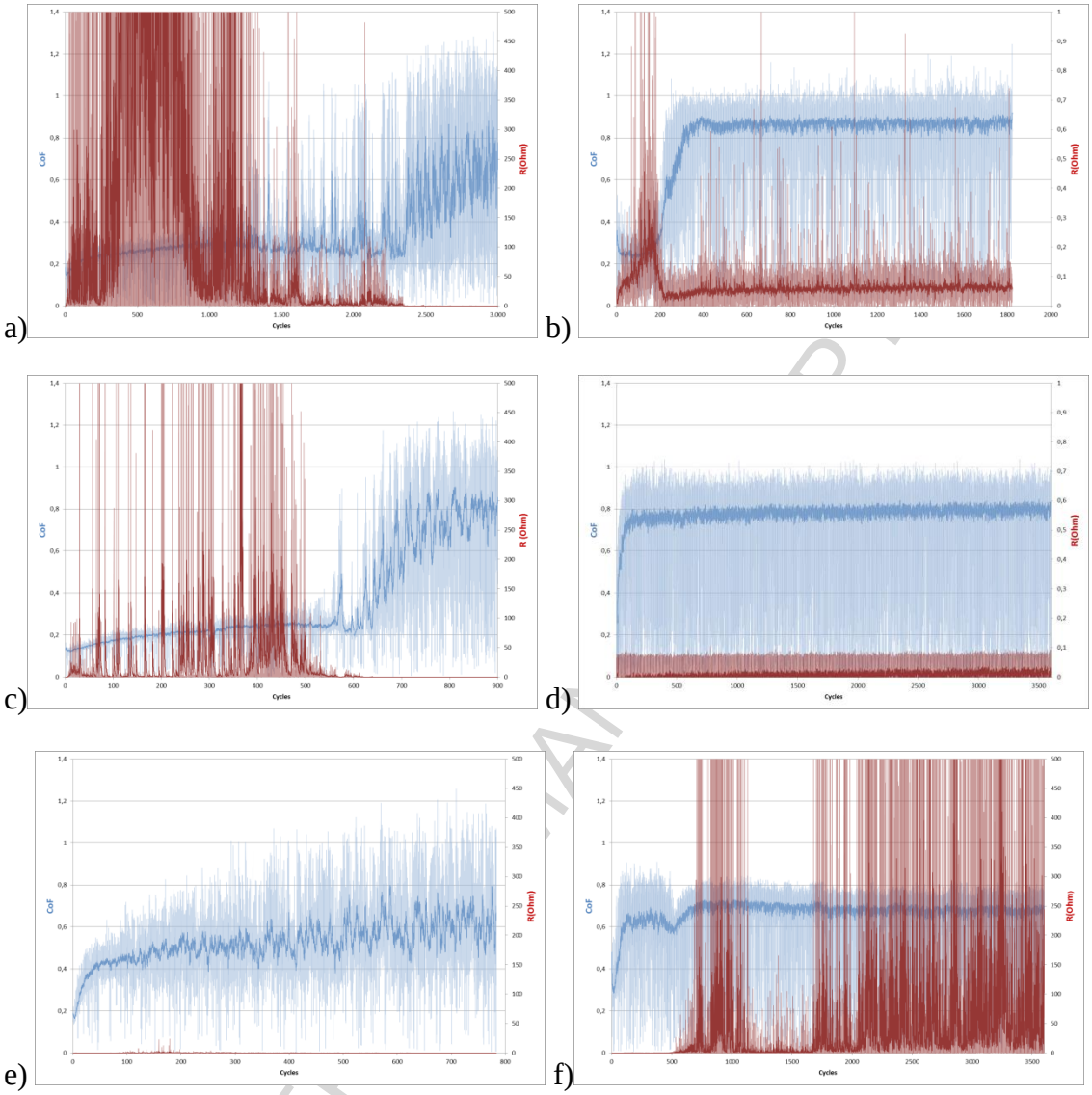

Fig. 6.

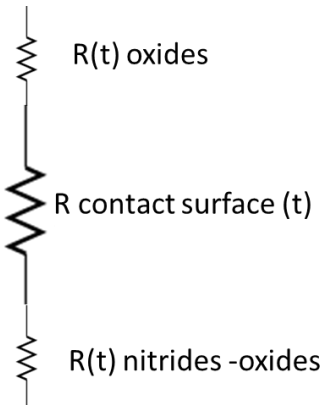

Fig. 7.

a) b)

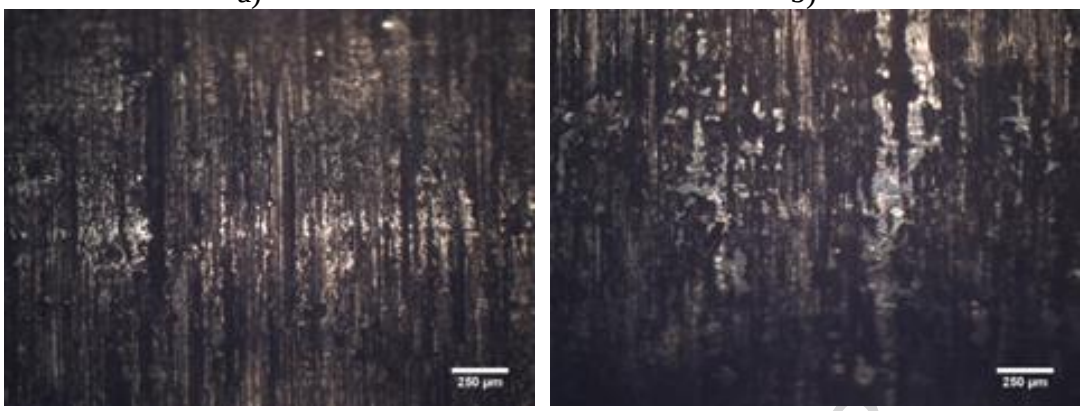

Fig. 8.

Acknowledgements

This work was supported the ProSurface project by MINECO (Spanish Ministry of Economy and Competitiveness) under grant No. RTC-2015-3595-4 and by the Economic Development Department at the Basque Government under Elkartek nG-17 grant.

Highlights

- Improvement of tribological features, without loss of corrosion resistance, in the 15-5PH martensitic stainless steel.
- Short treatment times with high density plasmas, based on active screen plasma and the hollow cathode effect.
- Surface status monitoring by Electrical Contact Resistance (ECR).